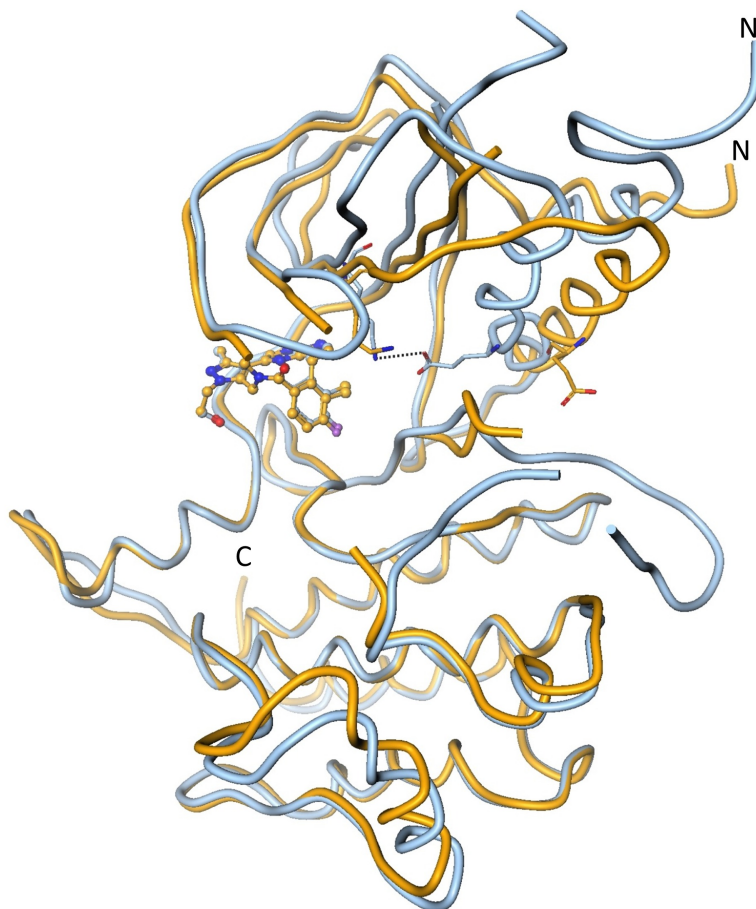
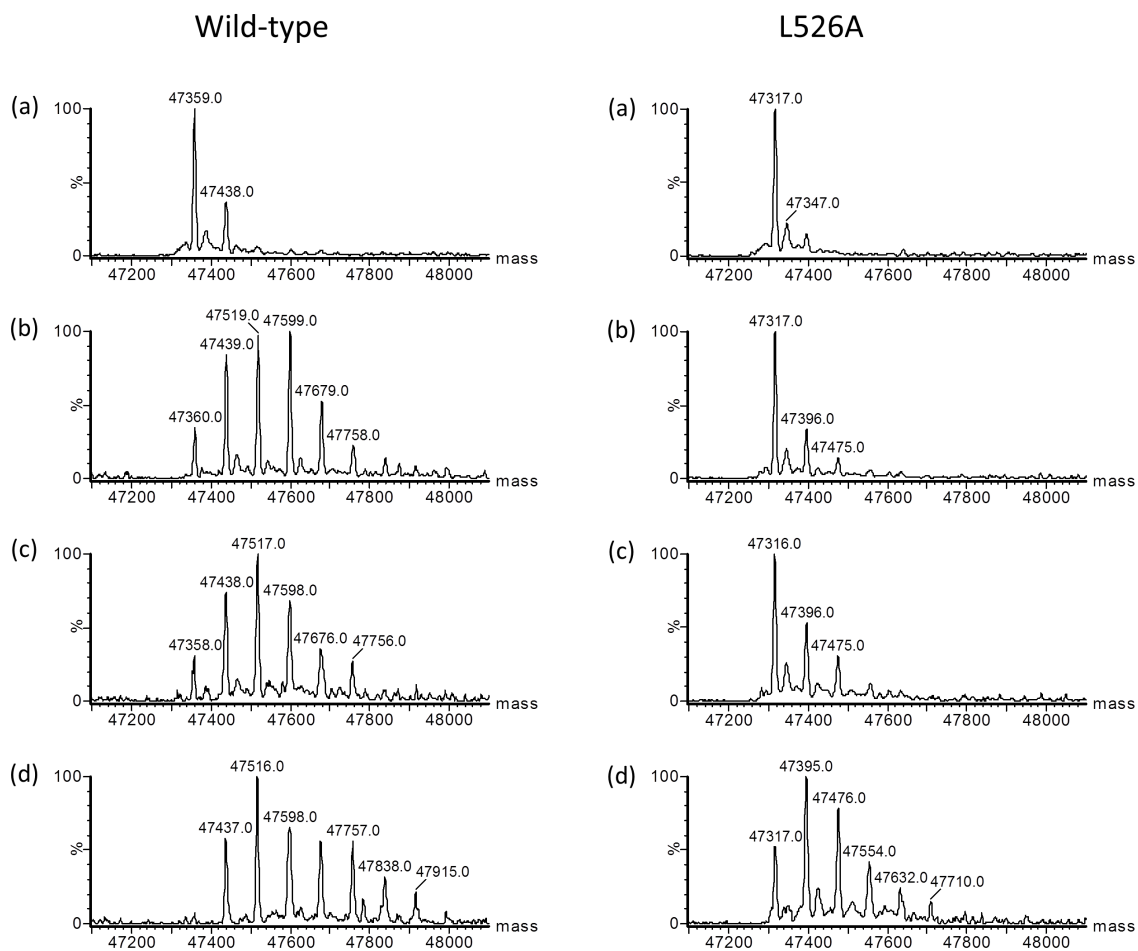


**Figure S1:** Electron density maps for the ligand and the hinge region of the protein. The experimental  $F_o - F_c$  maps contoured at  $3\sigma$  are shown for (a) Ax1 (protein shown in orange) and (b) Mer (protein shown in green). Corresponding stereo figures showing refined  $2F_o - F_c$  maps contoured at  $1\sigma$  are shown in (c) and (d).



**Figure S2:** Superposition of the two conformational states of the Axl kinase domain highlights the difference between the inactive (orange) and the active (blue) states.



**Figure S3:** MS analysis of the wild-type and L526A Axl (residues 473 - 894) autophosphorylation. (a) control (no ATP) (b) 5 min with ATP (c) 10 min with ATP and (d) 60 min with ATP. Measured molecular weight is shown. Predicted molecular weight for the wild-type Axl is 47366.9 Da and for L526A Axl is 47324.8 Da.

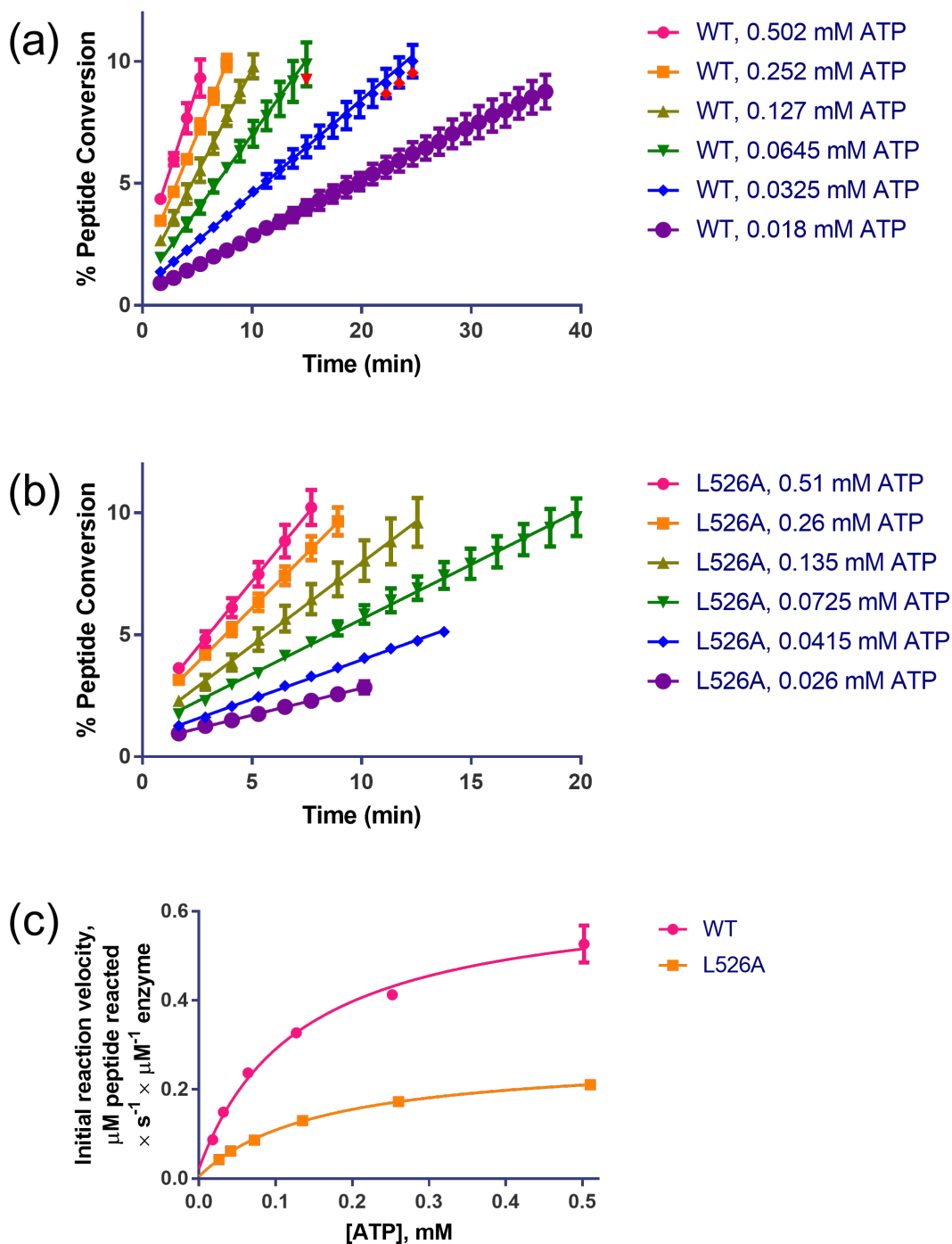


**Figure S4:** Enzyme kinetics of phosphorylation of 5-FAM-KKKKKEEIYFFF-CONH2 peptide by pre-activated wild-type and L526A Axl (residues 473 - 894) using a mobility-shift assay. Time courses of phosphorylation by (a) wild-type and (b) L526A Axl. (c) ATP-dependence of initial reaction velocities. The data was fitted to a Michaelis-Menten equation to determine apparent  $k_{\text{cat}} = 0.63 \pm 0.03 \text{ s}^{-1}$  (wild-type) and  $0.27 \pm 0.01 \text{ s}^{-1}$  (L526A), and apparent ATP  $K_M = 0.13 \pm 0.03 \text{ mM}$  (wild-type) and  $0.16 \pm 0.01 \text{ mM}$  (L526A), with  $3 \mu\text{M}$  5FAM-FL-Peptide30 as described in the Methods. The experiments were performed in duplicate.

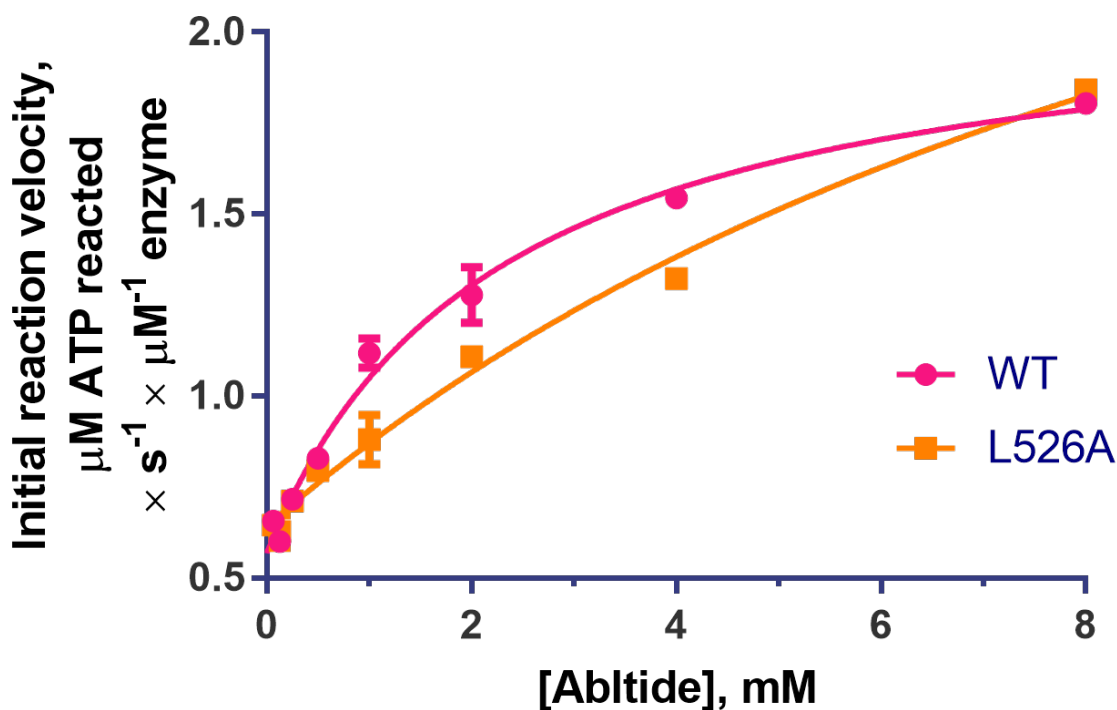


**Figure S5:** Enzyme kinetics of phosphorylation of Abltide substrate by pre-activated wild-type and L526A Axl (residues 473 - 894) in 1 mM ATP by a continuous spectrophotometric coupled enzyme assay. The assays were conducted in duplicate by following the oxidation of NADH in the presence of pyruvate kinase and lactate dehydrogenase coupled enzyme system, as described in the Methods, and fit to a Michaelis-Menten equation with a floating background to derive  $k_{\text{cat}} = 1.6 \pm 0.1 \text{ s}^{-1}$  and  $>0.8 \text{ s}^{-1}$  for the wild-type and L526A Axl, respectively, and  $K_{\text{M, Abltide}} = 2.2 \pm 0.3 \text{ mM}$  and  $>8 \text{ mM}$ , for wild-type and L526A Axl, respectively. Both proteins exhibited significant peptide-independent ATPase-like activity as evidenced from the y-intercept. The protein concentrations were adjusted as described in Methods to account for measured active site content of 26 % and 10 % for the wild-type and L526A Axl respectively .

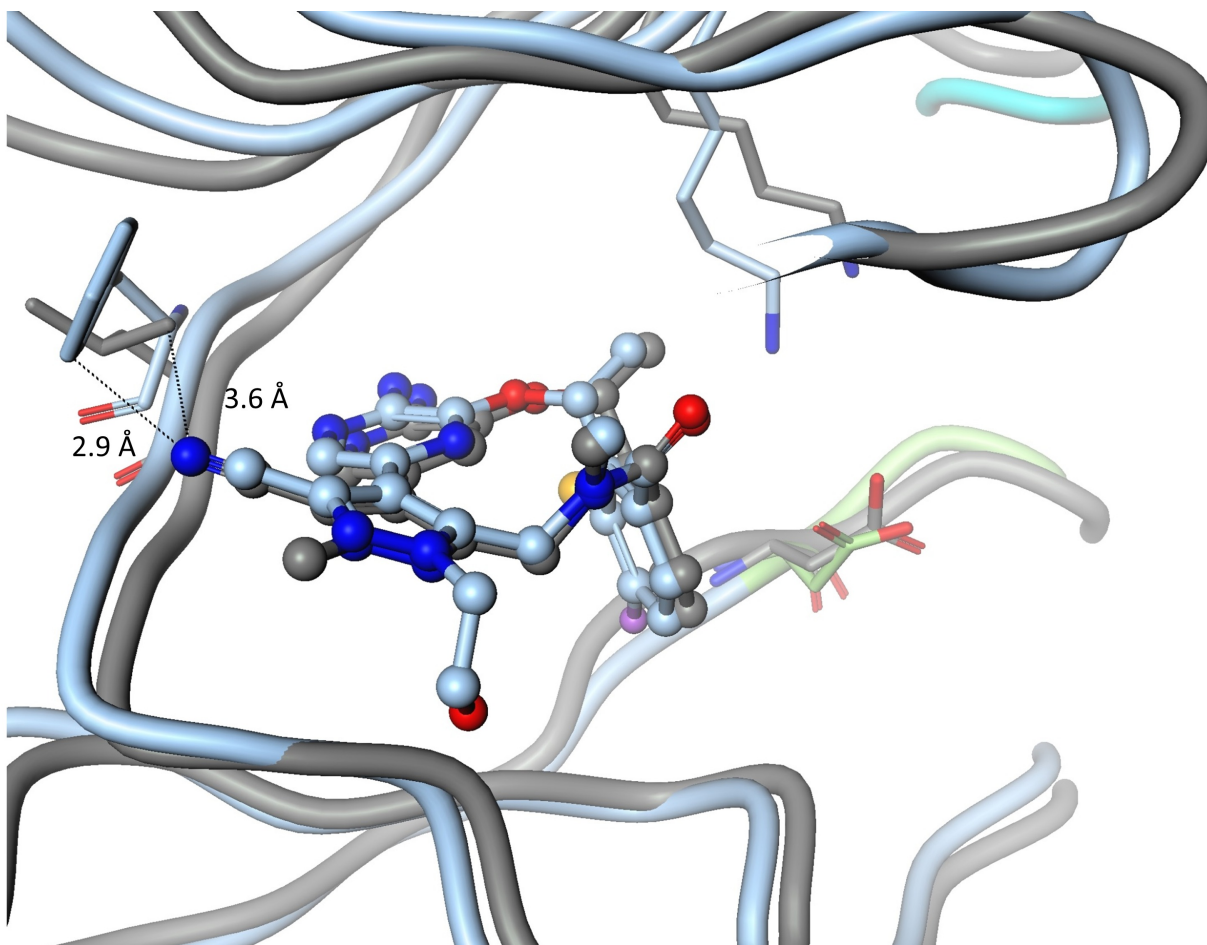


**Figure S6:** Comparison of the mode of recognition of compound 1 by Axl (blue) with that of lorlatinib by ALK (grey, PDBID: 4CLI). Nitrile on lorlatinib affords it selectivity over kinases that have an aromatic residue at the position equivalent to Leu1198 of ALK.

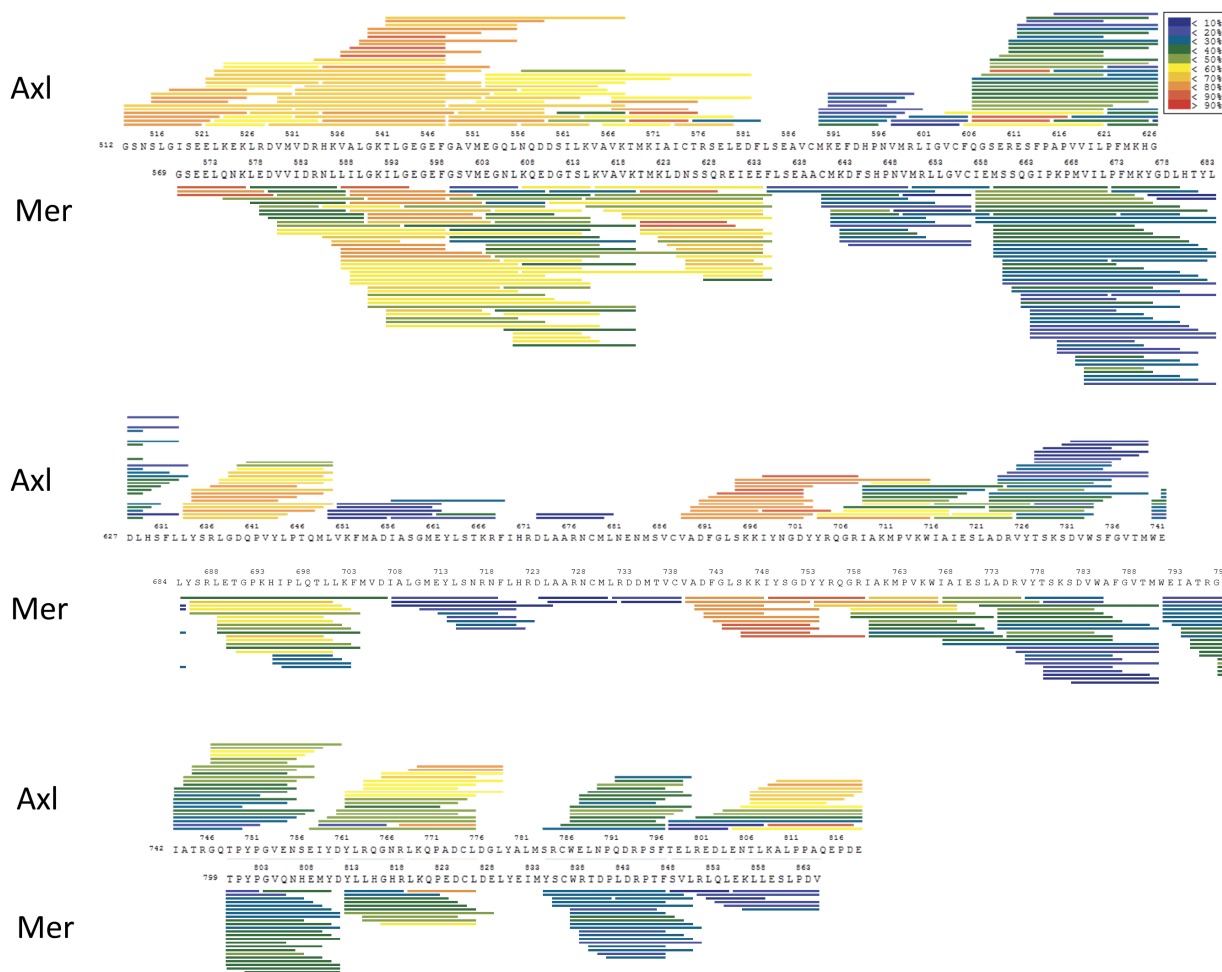


**Figure S7:** HDX-MS profiles of the Axl and Mer kinase domains. Deuterium exchange is color coded by the extent/percentage of peptide deuterium uptake, from blue < 10 % to red > 90 %. Higher deuterium exchange within the N-lobe observed for Axl, indicative of its heightened structural dynamics, generated a binomial isotopic envelope consistent exchange by EX2 kinetics. There is no indication of exchange by EX1 kinetics in the HDX-MS data. EX1 behavior is typically evident in broadened or bimodal isotopic envelopes upon exchange.